Anomalous flow of light near a photonic crystal pseudo-gap

Kyle M. Douglass,[1] Sajeev John,[2] Takashi Suezaki,[3,4] Geoffrey A. Ozin,[3] and Aristide Dogariu[1,*]

[1]*CREOL, The College of Optics and Photonics, University of Central Florida, 4000 Central Florida Boulevard, Orlando, FL 32816, USA*
[2]*Department of Physics, University of Toronto, 60 Saint George Street, Toronto, Ontario, M5S-1A7, Canada*
[3]*Department of Chemistry, University of Toronto, 80 Saint George Street, Toronto, Ontario, M5S-3H6, Canada*
[4]*Currently with the Kaneka Corporation, Japan*
[*]*adogariu@creol.ucf.edu*

Abstract: Two different transport regimes of light are observed in reflection from the same disordered photonic crystal. A model based on the scaling theory of localization explains the behavior of the path length-resolved reflection at two different probing wavelengths. Our results demonstrate the continuous renormalization of the photon diffusion coefficient measured in reflection from random media.

OCIS codes: (290.1990) Diffusion; (160.5293) Photonic bandgap materials.

References and links

1. A. Ishimaru, *Wave Propagation in Random Media* (John Wiley & Sons, 1999).
2. M. C. W. van Rossum and T. M. N. Nieuwenhuizen, "Multiple scattering of classical waves: microscopy, mesoscopy, and diffusion," Rev. Mod. Phys. **71**(1), 313–371 (1999).
3. Y. Kuga and A. Ishimaru, "Retroreflectance from a dense distribution of spherical particles," J. Opt. Soc. Am. A **1**(8), 831–835 (1984).
4. A. Z. Genack and A. A. Chabanov, "Signatures of photon localization," J. Phys. Math. Gen. **38**(49), 10465–10488 (2005).
5. F. Scheffold and G. Maret, "Universal conductance fluctuations of light," Phys. Rev. Lett. **81**(26), 5800–5803 (1998).
6. P. W. Anderson, "Absence of diffusion in certain random lattices," Phys. Rev. **109**(5), 1492–1505 (1958).
7. S. John and M. J. Stephen, "Wave propagation and localization in a long-range correlated random potential," Phys. Rev. B **28**(11), 6358–6368 (1983).
8. S. John, "Electromagnetic absorption in a disordered medium near a photon mobility edge," Phys. Rev. Lett. **53**(22), 2169–2172 (1984).
9. S. John, "Strong localization of photons in certain disordered dielectric superlattices," Phys. Rev. Lett. **58**(23), 2486–2489 (1987).
10. S. John and R. Rangarajan, "Optimal structures for classical wave localization: An alternative to the Ioffe-Regel criterion," Phys. Rev. B Condens. Matter **38**(14), 10101–10104 (1988).
11. M. Störzer, P. Gross, C. M. Aegerter, and G. Maret, "Observation of the critical regime near Anderson localization of light," Phys. Rev. Lett. **96**(6), 063904–063907 (2006).
12. D. S. Wiersma, P. Bartolini, A. Lagendijk, and R. Righini, "Localization of light in a disordered medium," Nature **390**(6661), 671–673 (1997).
13. T. Schwartz, G. Bartal, S. Fishman, and M. Segev, "Transport and Anderson localization in disordered two-dimensional photonic lattices," Nature **446**(7131), 52–55 (2007).
14. E. Abrahams, P. W. Anderson, D. C. Licciardello, and T. V. Ramakrishnan, "Scaling theory of localization: absence of quantum diffusion in two dimensions," Phys. Rev. Lett. **42**(10), 673–676 (1979).
15. C. Toninelli, E. Vekris, G. A. Ozin, S. John, and D. S. Wiersma, "Exceptional reduction of the diffusion constant in partially disordered photonic crystals," Phys. Rev. Lett. **101**(12), 123901 (2008).
16. P. W. Anderson, "The question of classical localization: a theory of white paint?" Philos. Mag. B **52**(3), 505–509 (1985).
17. M. S. Patterson, B. Chance, and B. C. Wilson, "Time resolved reflectance and transmittance for the non-invasive measurement of tissue optical properties," Appl. Opt. **28**(12), 2331–2336 (1989).
18. G. Popescu and A. Dogariu, "Optical path-length spectroscopy of wave propagation in random media," Opt. Lett. **24**(7), 442–444 (1999).
19. A. Blanco, E. Chomski, S. Grabtchak, M. Ibisate, S. John, S. W. Leonard, C. Lopez, F. Meseguer, H. Miguez, J. P. Mondia, G. A. Ozin, O. Toader, and H. M. van Driel; "Large-scale synthesis of a silicon photonic crystal with a complete three-dimensional bandgap near 1.5 micrometres," Nature **405**(6785), 437–440 (2000).

#156020 - $15.00 USD Received 11 Oct 2011; revised 14 Nov 2011; accepted 17 Nov 2011; published 28 Nov 2011

20. C. Conti and A. Fratalocchi, "Dynamic light diffusion, three-dimensional Anderson localization and lasing in inverted opals," Nat. Phys. **4**(10), 794–798 (2008).
21. P. M. Johnson, A. Imhof, B. P. J. Bret, J. G. Rivas, and A. Lagendijk, "Time-resolved pulse propagation in a strongly scattering material," Phys. Rev. E Stat. Nonlin. Soft Matter Phys. **68**(1), 016604 (2003).
22. J. X. Zhu, D. J. Pine, and D. A. Weitz, "Internal reflection of diffusive light in random media," Phys. Rev. A **44**(6), 3948–3959 (1991).

The propagation of light in a disordered medium is often modeled as a random walk of photons [1, 2]. This model inherently discards the wave nature of the light and instead describes the spreading of the energy in a manner similar to particles diffusing in a suspension. However, under certain conditions, interference effects between the multiply scattered waves within the medium will cause the random walk model to break down. Interference effects have been linked to a broad range of optical transport phenomena, including enhanced backscattering [3], transmittance fluctuations [4], and long range correlations [5], to name a few. A related phenomenon, that of Anderson localization [6], was first theorized for an electron in a disordered lattice. Localization was then generalized to all wave phenomena [7] and in particular to light [8]. In the case of light localization in a disordered photonic crystal, a new criterion for the localization transition has been postulated [9, 10].

Experimental work on light propagation in various disordered systems has revealed the subtleties involved in this field of study. Specifically, systems comprised of compressed TiO_2 powder [11], ground semiconductors [12], and planar photonic crystals [13] have all provided interesting and varied results. Many of these works derive their conclusions based on the scaling theory of localization [14] in which the optical diffusion coefficient is reduced as the size of the medium increases. For example, an argument based on the scaling theory was recently made to explain anomalies in the temporal shape of a pulse of light that was transmitted through a sample of compressed TiO_2 powder [11]. Other experiments in highly scattering systems found renormalized values for the diffusion coefficient without observing the renormalization process itself [15]. Although useful for quantifying results, the theory is not explicit about the dynamics of the diffusion process and lacks an intuitive description for the evolution of the optical energy as it propagates through the medium. Furthermore, all of the above experiments were carried out in transmission. To date, there is no experimental report on the scale-dependent nature of the diffusion coefficient close to the localization threshold in reflection. Here we report the observation of two different transport regimes of reflected, multiply scattered light from the same disordered photonic crystal and describe the interaction with a model based on the scaling theory.

To begin, imagine that an impulse of light (e.g. an ultrashort pulse) is incident on the surface of a slab of a random material of thickness L much smaller than the slab's transverse dimensions. The pulse will take on average a time to traverse the slab. The diffusion coefficient D describes the root mean square temporal spread of the photon density within the classical random walk model. Under the condition that the transport mean free path approaches the wavelength λ of light but L remains large compared to λ, the diffusion coefficient will decrease with L according to [8, 16]

$$D = \frac{v\ell}{3}\left(\frac{\ell}{\xi} + \frac{\ell}{L} + \frac{\ell}{L_{abs}}\right) \tag{1}$$

where v is the energy transport velocity and λ is the transport mean free path. The quantities ξ and L_{abs} are known as the coherence and root mean square (RMS) absorption length, respectively, and act as cutoff length scales for the scaling behavior of the diffusion coefficient. Equation (1) is the solution to the differential scaling equation obtained by incorporating coherent backscattering corrections to classical diffusive transport of the wave energy [14]. The coherence length is predicted to diverge with optical frequency as the frequency approaches a photon mobility edge. Anomalous transport is expected on length scales shorter than ξ, whereas on longer scales light resumes diffusive behavior with a

#156020 - $15.00 USD Received 11 Oct 2011; revised 14 Nov 2011; accepted 17 Nov 2011; published 28 Nov 2011

reduced diffusion coefficient. The classical diffusion coefficient $D_0 = v\ell/3$ can be recovered in the limit that the coherence length approaches the value of the transport mean free path and the system size and absorption lengths become large.

The diffusion coefficient D is related to the RMS displacement R of the energy by $R = \sqrt{6Dt}$. When D is independent of R itself, the diffusion process is considered "normal". However, when interference causes D to decrease with R the process is called subdiffusive. Our measurements support the hypothesis that, in reflection, R represents the effective size L of the system seen by the light as illustrated in Fig. 1. This makes the reflection geometry unique; in transmission, the system size is always set by the physical thickness of the medium. If we identify R with L in Eq. (1), then for $R << \xi$ and L_{abs}, Eq. (1) and the original relation between R and time predicts that $R^3 = 6(D_0\ell)t$.

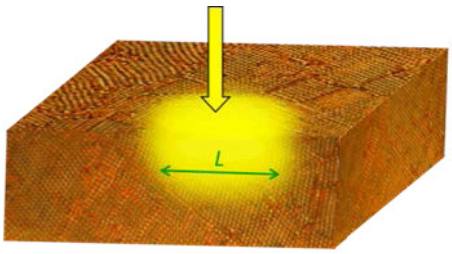

Fig. 1. The RMS displacement of the diffuse light from a source determines the effective size L of the material seen by the light.

From the theory of optical diffusion, one can calculate the expression for the time-resolved, backscattered photon flux across the surface of a semi-infinite disordered medium. The flux at the surface directly above an isotropic point source is [17]

$$p(t) = (4\pi D)^{-3/2} z_0 z_e t^{-5/2} \times \exp(-\mu_{abs} v t) \exp\left[\frac{-(z_0 z_e)^2}{4Dt}\right] \qquad (2)$$

where μ_{abs} is the absorption coefficient and z_0 is the depth of the point source inside the medium, usually taken to be one transport mean free path. The extrapolation length ratio z_e represents the distance (as a fraction of z_0) outside of the medium at which the photon density goes to zero. All other quantities retain their previous meanings.

From Eq. (2), the time-resolved photon flux depends on D and, consequently, contains information about the behavior of the RMS displacement of the energy. After taking the logarithm of both sides, one obtains

$$\log[p(t)] = -\frac{3}{2}\log(D) - \frac{5}{2}\log(t) - 2\mu_{abs} v t - \frac{(z_0 z_e)^2}{4Dt} + const. \qquad (3)$$

The term describing the flux close to the boundary $\left[-(z_0 z_e)^2/4Dt\right]$ can be neglected for sufficiently long times. Furthermore, for times before the absorption becomes significant, one can neglect the third term as well. It follows that, when D is constant, the photon flux will decay with t according to a power law with an exponent −5/2. This behavior is valid only in the regime noted above, and is indeed observed in the diffuse reflectance from many relatively weak, multiple scattering materials such as suspensions of polystyrene microspheres in water (c.f. Figure 2) [18]. On the other hand, in the presence of scaling effects Eq. (2) will be modified as follows. Starting from Eq. (1), using the relation between the RMS displacement and system size, and neglecting the absorption losses, one easily finds that the diffusion coefficient D is given by

#156020 - $15.00 USD Received 11 Oct 2011; revised 14 Nov 2011; accepted 17 Nov 2011; published 28 Nov 2011

$$D = D_0 \ell \left(\frac{1}{\xi} + \frac{1}{\sqrt{6Dt}} \right). \tag{4}$$

Here $D_0 = v\ell/3$ is the diffusion coefficient in the absence of scaling. When the RMS displacement is much smaller than the coherence length ξ such that the first term in the sum of Eq. (4) is insignificant, the diffusion coefficient exhibits a scaling behavior like $D \sim t^{-1/3}$. We emphasize here that the diffusion coefficient for a given photon does not vary with time. Instead, photons that are associated with a larger RMS displacement of the energy have a smaller (renormalized) diffusion coefficient. This fact is demonstrated later by the results of a transmission experiment in which no time dependent diffusion coefficient was observed.

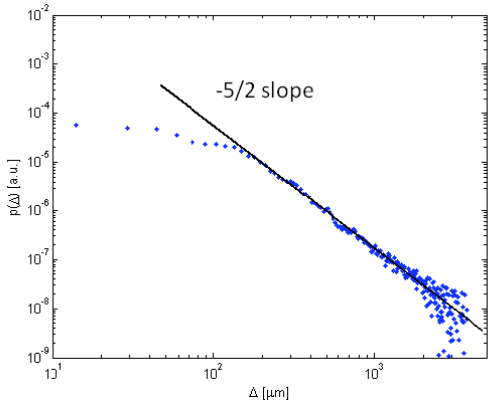

Fig. 2. Path length distribution measured in reflection for a semi-infinite medium comprising a suspension of 0.43 μm diameter polystyrene spheres in water. The −5/2 slope on a log-log scale is indicative of normal diffusion.

In these conditions, after substituting Eq. (4) into Eq. (3) one obtains

$$\log\left[p(t) \right] \cong -2\log(t) + const. \tag{5}$$

This significant result predicts that any scaling effects will cause the decay of the photon flux to exhibit a power law dependence with a −2 exponent. Once the extent of the diffuse light has grown past the cutoff length scale imposed by ξ, one should expect a return to a −5/2 exponent and an eventual exponential decay due to absorption losses or finite sample sizes.

To test the scale-dependent diffusion hypothesis we explored optical diffusion in a disordered 3D silicon inverse-opal photonic crystal [19]. The presence of disorder in photonic crystals can induce a severe reduction in the electromagnetic density of states (DOS) and provides an ideal situation for the observation of scaling effects [8, 20]. To this end we employed optical path length spectroscopy (OPS) [18] to obtain photon path length distributions from the sample. The experimental setup is illustrated in Fig. 3 and consists of a fiber-based Michelson interferometer with a superluminescent LED as the source. A single-mode fiber in one arm of the interferometer both injects and collects light from the sample. Due to the low coherence length of the source, interference between the two arms is observed only for backscattered light that has traveled a distance equivalent to twice the reference arm length, which is adjusted by a scanning mirror. The envelope of this interference signal is computed and corresponds to a path length distribution for one material realization. In principle, OPS provides the same information as that obtained in time-of-flight experiments [21]. A simple transformation from the mirror displacement, Δ, to time allows for a direct comparison between the two techniques. The simplicity of OPS and, most importantly, the single mode of operation for both emission and detection allow for an easy assessment of reflection type measurements.

#156020 - $15.00 USD Received 11 Oct 2011; revised 14 Nov 2011; accepted 17 Nov 2011; published 28 Nov 2011

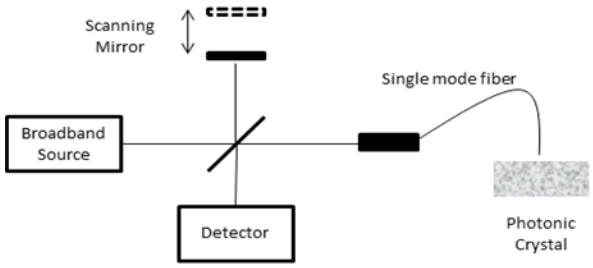

Fig. 3. Fiber-based Michelson interferometer used for collection of photon path length distributions from multiple scattering media. The single-mode fiber acts as both a source and detector.

We collected path length distributions from a disordered photonic crystal at two different wavelengths. The silicon inverse opal was grown under conditions leading to a large number of imperfections and is similar to those reported in Ref [15]. Light microscopy images of the sample revealed both small and large scale (tens to hundreds of lattice constants) lattice dislocations and variations in the normal-facing crystal plane. The path length distributions were recorded while slowly displacing the sample on a moveable stage beneath the probe fiber for 50 scans of the scanning mirror. All scans were averaged over the ensemble of path length distributions. The fiber was positioned at approximately 1 mm above the surface of the sample. No significant differences were observed for heights ranging from 200 μm to 1 *mm*. The fiber was also oriented at a slight angle with respect to the normal of the sample face to reduce the amount of single-scattered light reflected from the sample's glass substrates. Furthermore, the impulse response of the entire system was subtracted from the origin of each distribution in order to reduce any ambiguity due to specular reflection from the surface. The two light sources that were used in our study had wavelengths of 1300 *nm* and 1550 *nm* and coherence lengths of 34 ± 2 μm and 38 ± 1 μm, respectively. The thickness of the sample was measured using a profilometer and was 15.0 ± 2.7 μm.

Figure 4(a) depicts a typical averaged path length distribution as a function of Δ. The sample displays diffusive and scaling behaviors for excitations at 1300 *nm* and 1550 *nm*, respectively. The solid lines have been drawn on the graph as an aid to the eye. The power law with an exponent of −2 is a clear indication of a continuous renormalization of the diffusion coefficient when excited with 1550 *nm* light. It is worth noting that no other physical effect (e.g. absorption or finite sample size) can cause an increase in the slope from −5/2 to −2. The path length distributions collected from light with a wavelength of 1550 nm systematically decayed slower with path length over the regions of interest (Δ spanning 0 to ~600 microns) than distributions from light with a wavelength of 1300 nm.

#156020 - $15.00 USD Received 11 Oct 2011; revised 14 Nov 2011; accepted 17 Nov 2011; published 28 Nov 2011

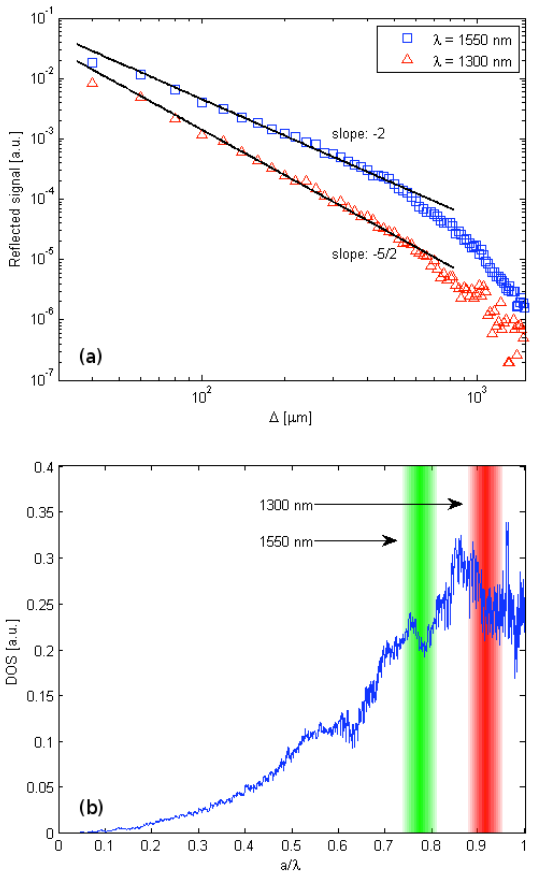

Fig. 4. (a) Path length distribution of reflected photon path lengths from the disordered photonic crystal. (b) Estimated density of states for the sample. Shaded bands indicate the spectral regions that were probed. The widths of the bands are related to the uncertainty in the lattice constant, *a*.

The choice of wavelengths used in our measurements was made by considering the estimated density of states (DOS) as shown in Fig. 4(b). Band diagrams were calculated for thirteen different inverse opals whose structures were determined by three free parameters: the refractive index of silicon (ranging between 3.4 and 3.6), the ratio of the air hole diameter to the lattice constant (0.355 to 0.38), and the ratio of the outer diameter of the silicon spheres to the lattice constant (0.39 to 0.41) [19]. The values of the parameters for each structure were randomly chosen from the given ranges and represent realistic values and variations in our structure. Each band diagram was then numerically integrated in k-space over the first Brillouin zone to obtain the DOS for that structure. The final DOS estimate in Fig. 4(b) was obtained by averaging all thirteen structures. As can be seen, a pseudo-gap in the DOS at 1550 *nm* survives the averaging and explains why renormalization is observed at this wavelength. The DOS at 1300 *nm* is larger than at 1550 *nm* and is more sensitive to the structural parameters, resulting in more uncertainty in the estimate. The sample is effectively random at this wavelength and no longer displays crystalline properties.

Some of the relevant transport parameters were estimated from the measurements. In doing so we assumed an exponential loss due to absorption with a characteristic length of $\Delta_{abs} = 3000\ \mu m$ at both wavelengths. This value is consistent with Ref [15], in which a characteristic absorption time of $\tau_{abs} = 20\ ps$ was found. To fit the data at 1300 nm, we used the classical diffusion result in Eq. (2) and a least-squares fitting routine with an extrapolation

#156020 - $15.00 USD Received 11 Oct 2011; revised 14 Nov 2011; accepted 17 Nov 2011; published 28 Nov 2011

length $z_e = 1.6$. This value was estimated according to Ref [22]. for an averaged refractive index and the air-to-silicon filling fraction for our samples. The range of the fits included the second data point up to the one closest to 500 μm. The resulting value for D at 1300 nm was $35.6 \pm 8.9\ m^2/s$. The uncertainty is due to the finite coherence length of the light source. For data collected at 1550 nm, we used the same expression for the flux but with a diffusion coefficient depending on Δ as given in Eq. (4). Two fitting parameters, ξ and λ, were used in this case. An initial diffusion coefficient D_0 (before scaling effects begin) was then calculated with an assumed transport velocity of $v = 3\times10^7\ m/s$, as justified previously [15]. The value for D_0 is $25.5 \pm 6.8\ m^2/s$. In this case we estimated $z_e = 2.5$ based on the surface reflectivity measured at the two wavelengths and following again the procedure of Ref [22]. The corresponding value for ξ was found to be 13.6 ± 1.8 μm. Inserting these values into Eq. (1) together with the effective sample lengths $L_e = L + 2z_e\ell$ and neglecting the absorption cutoff, one can obtain the value for the renormalized diffusion coefficient: 7.4 ± 4.0 m^2/s. This is the diffusion coefficient that would appear in path length-resolved transmission measurements. The reported uncertainty reflects both the fluctuations in the sample's thickness and the effect of the finite coherence lengths of the sources.

The significance of reflection measurements can be made further apparent by examining the behavior of transmitted, path length-resolved (or time-resolved) photons from our sample. Figure 5 depicts the equivalent time dependence of light transmittance through the sample. The data were collected by a modified OPS setup in which light from one arm of a fiber circulator was focused onto the sample and the fiber from another arm collected the light from the opposite surface. The data were then scaled onto the appropriate time axis. The slopes of the long time exponential decays were used to calculate the diffusion coefficient [21]. We found the values of 49.7 ± 8.1 m^2/s and 3.9 ± 0.6 m^2/s for wavelengths of 1300 *nm* and 1550 *nm*, respectively. The value for D at 1550 *nm* agrees with the renormalized value estimated from reflection measurements, yet the behavior of the transmission data alone does not indicate that renormalization of the diffusion coefficient occurred. This is because a transmission experiment enforces the interaction with the entire medium. Photons arriving at different times (or path lengths) may have undergone different transport processes but this information is lost since every measured photon has necessarily traveled at least the sample thickness. Alternatively, a transmission experiment integrates over different scattering regimes.

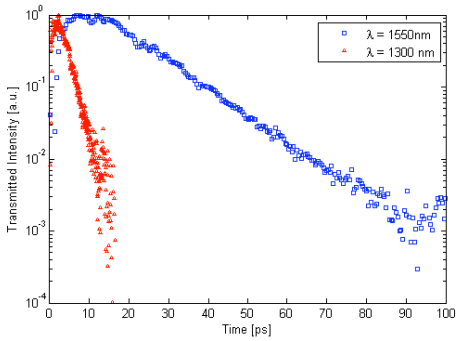

Fig. 5. Time of flight distributions measured in transmission at the two different wavelengths. The linear dependence on a semilog scale indicates that the diffusion coefficient depends on the size of the system, not time.

In conclusion, we presented a simple model for optical subdiffusion in random media. The model explains the observed behavior of the path length distributions for photons traveling in disordered photonic crystals before the onset of loss. We have shown that the diffusion of the photons slows down and causes a relative increase in the probability of photons existing at

#156020 - $15.00 USD Received 11 Oct 2011; revised 14 Nov 2011; accepted 17 Nov 2011; published 28 Nov 2011

longer path lengths relative to shorter ones when compared to the case of normal diffusion. The power law decay with an exponent of −2 is a clear indication that the diffusion coefficient is being continuously renormalized. In contrast, a normal diffusion process is characterized by a −5/2 power law decay.

We emphasize that our experiments were performed on exactly the same medium at two different wavelengths and demonstrate that structural disorder can induce vastly different spectral responses of the diffuse light. The present measurements provide the first conclusive evidence of scaling effects of light in reflection and suggest that the extent of the diffuse photon cloud in the medium can be interpreted as an effective system size.

#156020 - $15.00 USD Received 11 Oct 2011; revised 14 Nov 2011; accepted 17 Nov 2011; published 28 Nov 2011